Deep Learning-Based Cancer Diagnosis Using a Bluefin Trevally-Optimized Convolutional Neural Network

A. Kaliappan
School of Computing, SRM Institute of Science and Technology, Tiruchirappalli, Tamil Nadu, India
kaliappantpr@gmail.com

Subhasini Shukla
Electronics & Computer Science Engineering, St. John College of Engineering & Management, Palghar, Maharashtra, India
subhasinish@sjcem.edu.in

Rahul Nandkumar Khadke
Department of Electronics & Telecommunication, Aditya Engineering College, Beed, Maharashtra, India
khadke.rahul011@gmail.com

Ganesh B. Dongre
Department of Electronics and Computer Engineering, CSMSS Chh. Shahu College of Engineering, Chhatrapati Sambhajinagar, MH, India
ganeshbdongre@gmail.com

Robin George
Institute of Science and Technology, Chinmaya Vishwa Vidyapeeth, Ernakulam, Kerala, India
robin.george@cvv.ac.in

Nitesh N Nikam
Department of Electrical Engineering, CSMSS Chh. Shahu College of Engineering, Chhatrapati Sambhajinagar, MH, India
niteshnikam1408@gmail.com

R. D. Prathibha
Department of Zoology, St. Joseph's University, Bengaluru, India
Prathiba@sju.edu.in

M. R. Amruthalakshmi
Department of Mathematics, Dayananda Sagar College of Engineering, Bengaluru, India
amruthamirajkar@gmail.com

B. Aruna
Department of Electronics and Communication Engineering, BGS Institute of Technology, Adichunchanagiri University, B G Nagara, Mandya, Karnataka, India
baruna@bgsit.ac.in

Madhumathi R.
Department of Computer Science and Engineering, Sri Ramakrishna Engineering College, Coimbatore, India
madhumathi.r@srec.ac.in

Awwab Mohammad
Department of Computer Science and Technology, Manav Rachna University, Faridabad, India
awwabmohammad92@gmail.com (corresponding author)

Received: 22 January 2026 | Revised: 7 February 2026 and 18 February 2026 | Accepted: 19 February 2026

 DOI: https://doi.org/10.48084/etasr.17713

ABSTRACT

Accurate and automated detection of brain tumors from Magnetic Resonance Imaging (MRI) scans is critical for effective clinical diagnosis and treatment planning. This paper proposes a Bluefin Trevally Optimization-based Deep Learning (BTO-DL) framework for robust brain tumor detection and analysis from MRI images. The proposed approach integrates a Convolutional Neural Network (CNN)–based feature extraction with a bio-inspired Bluefin Trevally Optimization (BTO) algorithm to jointly optimize network hyperparameters and feature importance weights, thereby enhancing convergence stability and generalization performance. The framework was tested on several publicly available benchmark brain MRI datasets, such as BraTS, Figshare, and Kaggle. It was trained over 50 epochs and used a patient-independent data split, demonstrating superior classification accuracy, spatial overlap, and convergence stability compared to existing methods. On the BraTS dataset, it achieves a classification accuracy of over 98%, Receiver Operating Characteristic–Area Under the Curve (ROC–AUC) values close to 0.99, and a Dice coefficient of 0.91. The model also shows stable training convergence, strong cross-dataset generalization, and low inference latency of about 18.6 ms per MRI slice indicating suitability for real-time clinical applications. A statistical significance test shows that the observed performance improvements are statistically significant ($p < 0.01$). The proposed BTO-DL framework offers a precise, efficient, and resilient solution for the automated detection and localization of brain tumors from MRI scans.

Keywords-brain tumor detection; MRI; deep learning; Bluefin Trevally Optimization (BTO); Convolutional Neural Network (CNN); Dice coefficient

I. INTRODUCTION

Brain tumors are one of the most serious neurological disorders because they can cause serious illness and death if not detected and treated early. Accurate and timely diagnosis is critical, and magnetic resonance imaging (MRI) is widely regarded as an effective diagnostic tool because of its high spatial resolution and superior soft-tissue contrast [1]. This need for precise diagnosis has led to the development of reliable and automated computer-aided diagnosis systems for detecting and analyzing brain tumors. Deep learning methods, especially Convolutional Neural Networks (CNNs), have demonstrated excellent performance in medical image analysis tasks in recent years, including brain tumor classification and segmentation [2]. CNN-based models can learn hierarchical feature representations directly from raw MRI data, eliminating the need for manual feature extraction. However, deep learning models are highly sensitive to hyperparameter selection, network architecture, and feature relevance [3]. Traditional methods often use manual tuning or trial-and-error methods, which are computationally expensive, suboptimal, and likely to lead to local minima. To overcome these constraints, bio-inspired and metaheuristic optimization techniques have been increasingly integrated with deep learning frameworks to automate hyperparameter selection and enhance model generalization [4].

This paper presents a framework for automated brain tumor detection from MRI scans called Bluefin Trevally Optimization-based Deep Learning (BTO-DL). The proposed optimization strategy simultaneously optimizes both CNN hyperparameters and feature importance weights. This is based on the coordinated hunting and adaptive movement behavior of bluefin trevally fish. The framework was evaluated on several publicly available benchmark brain MRI datasets, including BraTS, Figshare, and Kaggle, demonstrating effective performance and generalization across datasets.

Authors in [5] developed a hybrid Vision Transformer (ViT) and Gated Recurrent Unit (GRU) model for brain tumor classification, achieving high accuracy on multi-class MRI datasets. However, performance remained sensitive to the hyperparameter selection. Authors in [6] employed pre-trained CNN models with transfer learning for advanced brain tumor classification, demonstrating robust classification performance across datasets. However, they reported reduced performance for infiltrative tumor regions because the boundaries weren't the same everywhere. To address CNN limitations in specific scenarios, authors in [7] proposed a CNN–Transformer hybrid framework, increasing Dice coefficients on BraTS data to approximately 0.89, but at the cost of higher computational complexity. Authors in [8] used transfer learning with EfficientNet variants for classification, achieving 96–97% accuracy on contrast-enhanced MRI datasets. They also

emphasized the challenge of maintaining robustness on different scanners.

Metaheuristic-assisted deep learning has also gained attention. Authors in [9] applied deep learning techniques with optimization strategies for brain tumor classification and achieved accuracy improvements of 1–2% over baseline CNNs, although convergence instability was observed in some runs. Similarly, authors in [10] developed a hybrid AlexNet–GRU model for brain tumor classification, achieving high F1-scores while addressing computational efficiency, but at the expense of increased training time. More recently, authors in [11] incorporated explainability mechanisms such as Grad-CAM into deep classification models, achieving accuracies above 97% while improving interpretability, yet still relying on manually tuned optimization strategies.

The proposed BTO-DL framework addresses these limitations by combining bio-inspired optimization with CNN feature learning to provide an efficient and reliable solution for automated brain tumor detection from MRI scans.

II. METHODOLOGY

This section describes the proposed BTO-DL framework for brain tumor detection from MRI scans.

A. Problem Definition

Let the brain MRI dataset be defined as:

$$\mathcal{D} = \{(X_i, y_i)\}_{i=1}^{N} \quad (1)$$

where N denotes the total number of MRI samples, $X_i \in \mathbb{R}^{H\times W\times C}$ represents the i^{th} MRI image with height H, width W, and C MRI modalities (e.g., T1, T2, FLAIR), and $y_i \in \{1,2,\dots,K\}$ is the corresponding tumor class label.

The objective of the proposed framework is to learn a discriminative function:

$$f_\theta: X \to y \quad (2)$$

where f_θ is a deep CNN parameterized by θ, such that the predicted label $\hat{y}_i = f_\theta(X_i)$ closely matches the ground truth y_i.

B. MRI Preprocessing

Preprocessing is applied to reduce scanner-dependent intensity variations and enhance tumor-related structures.

1) Intensity Normalization

Each MRI image is normalized using z-score normalization:

$$X_i^{norm} = \frac{X_i - \mu(X_i)}{\sigma(X_i)} \quad (3)$$

Here, $\mu(X_i)$ and $\sigma(X_i)$ represent the mean and standard deviation of pixel intensities of the i^{th} image, respectively. Equation (3) ensures that all images have zero mean and unit variance, improving training stability and convergence.

2) Noise Suppression

To reduce high-frequency noise, Gaussian filtering is applied:

$$X_i^{denoise}(p) = \sum_{q\in\Omega} X_i^{norm}(q) \cdot G(p-q) \quad (4)$$

In (4), p is the target pixel, q represents the neighboring pixels in window Ω, and $G(\cdot)$ is a Gaussian kernel. This operation smooths out small changes in intensity while keeping the edges of the tumor [12].

C. Deep Feature Extraction

A CNN is employed to extract hierarchical spatial features from the preprocessed MRI images.

1) Convolutional Feature Mapping

At the l^{th} convolutional layer, feature maps are computed as:

$$F_l = \sigma(W_l * F_{l-1} + b_l) \quad (5)$$

where W_l and b_l denote the convolution kernel and bias, respectively; F_{l-1} is the input feature map from the previous layer; $*$ represents the convolution operation; and $\sigma(\cdot)$ is the ReLU activation function. Equation (5) allows the network to learn nonlinear features that are important for distinguishing tumor patterns [13].

2) Feature Vector Formation

Global Average Pooling (GAP) compresses spatial feature maps into a compact representation:

$$\mathrm{z}_i = [z_{i1}, z_{i2}, \dots, z_{id}] \quad (6)$$

Here, d represents the number of dimensions in the deep feature vector. Equation (6) reduces model complexity and the risk of overfitting while keeping important tumor features.

D. Bluefin Trevally Optimization

Bluefin Trevally Optimization (BTO) is a bio-inspired metaheuristic capable of simultaneously optimizing CNN hyperparameters and feature importance weights. Brain tumor MRI classification involves a high-dimensional, non-convex optimization landscape with strong parameter interdependencies. BTO's adaptive hunting strategy allows agents to dynamically shift between global exploration and local exploitation, making it well suited for such complex optimization problems. The essential parameters of BTO were empirically selected based on preliminary experiments and are summarized as follows: population size = 30 agents, maximum iterations = 50, learning rate bounds $\alpha \in [0.0001, 0.01]$, convolution kernel size $k \in \{3,5\}$, number of filters $n_f \in [32,128]$, and dropout ratio $\rho \in [0.2,0.5]$. These values provided a good trade-off between convergence stability and computational efficiency.

1) Solution Representation

Each Bluefin Trevally agent encodes a candidate solution:

$$\mathrm{S}_j = [\alpha, k, n_f, d_r, w] \quad (7)$$

where α is the learning rate, k is the kernel size, n_f is the number of convolutional filters, d_r is the dropout ratio, and w is the feature weight vector. Equation (7) enables BTO to optimize architectural and training parameters concurrently [14].

2) Feature Weighting Mechanism

The optimized feature vector is obtained via element-wise multiplication:

$$\tilde{z}_i = w \odot z_i \quad (8)$$

Equation (8) assigns adaptive importance to each feature dimension, enhancing tumor-relevant representations and suppressing redundant features [15].

3) Fitness Function Design

The quality of each candidate solution is evaluated using:

$$\mathcal{F}(S_j) = \lambda_1 \cdot Acc + \lambda_2 \cdot F1 - \lambda_3 \cdot \mathcal{L} \quad (9)$$

In (9), Acc denotes classification accuracy, $F1$ represents the harmonic mean of precision and recall, and $\mathcal{L}$ is the cross-entropy loss. Coefficients $\lambda_1, \lambda_2, \lambda_3$ control the contribution of each term, ensuring balanced optimization.

4) BTO Position Update Strategy

a) Exploration Phase

During global search, agent positions are updated as:

$$S_j^{t+1} = S_j^t + r_1(S_{best}^t - S_j^t) \quad (10)$$

Here, r_1 is a random number uniformly distributed in [0,1]. Equation (10) encourages diverse exploration by moving agents toward promising regions.

b) Exploitation Phase

Local refinement is achieved using:

$$S_j^{t+1} = S_{best}^t + r_2 \mid S_{best}^t - S_j^t \mid \quad (11)$$

Here, r_2 is a random number uniformly distributed in [0,1]. Equation (11) intensifies the search near the optimal solution [16]. While BTO shares superficial similarities with swarm-based optimizers in terms of population-based search, its update equations differ fundamentally by incorporating adaptive prey-encirclement and coordinated pursuit dynamics. Unlike PSO's velocity-based formulation, BTO directly modifies agent positions using biologically inspired collective movement, leading to smoother convergence trajectories and improved robustness against local optima [17].

5) Comparison with Existing Metaheuristic Optimizers

Unlike Particle Swarm Optimization (PSO), which relies on velocity-based updates, and Genetic Algorithms (GA), which use crossover and mutation, BTO is inspired by coordinated hunting and adaptive schooling behavior.

E. Classification Layer

1) Softmax Probability Estimation

The final class probabilities are computed using:

$$P(y = k \mid X) = \frac{e^{u_k}}{\sum_{j=1}^{K} e^{u_j}} \quad (12)$$

Equation (12) ensures normalized probabilities across K tumor classes.

2) Loss Function

The cross-entropy loss guiding network training is defined as:

$$\mathcal{L}_{CE} = -\sum_{k=1}^{K} y_k \log P(y = k \mid X) \quad (13)$$

Equation (13) penalizes incorrect predictions, enabling effective gradient-based learning [18].

III. RESULTS

The proposed BTO-DL framework was tested on several benchmark brain MRI datasets to evaluate its performance, robustness, and generalization capability.

A. Dataset Description

For all datasets, the data were split into three parts: 70% for training, 15% for validation, and 15% for testing. The model was trained for 50 epochs to ensure sufficient convergence. The BraTS dataset [19] contains multi-modal MRI scans (T1, T1c, T2, and FLAIR) labeled by expert radiologists and was used to classify tumor regions into high-grade and low-grade gliomas. The Figshare Brain MRI dataset [20] contains 3,064 T1-weighted contrast-enhanced MRI slices grouped into glioma, meningioma, pituitary tumor, and normal categories, enabling evaluation of model performance on visually similar tumor types. The Kaggle Brain MRI dataset [21] comprises approximately 7,000 MRI images from different sources and scanners and was used to assess if the model can identify the difference between tumors and non-tumors in different imaging conditions.

B. Performance Evaluation

Table I summarizes the performance on the Figshare Brain MRI dataset, which is also illustrated in Figure 1. The high Area Under the Curve (AUC) values shown in Table II for the Kaggle MRI dataset indicate that tumor and non-tumor classes are very well separated. Table III presents class-wise performance metrics (precision, recall, and F1-score) for each tumor category on the Figshare Brain dataset.

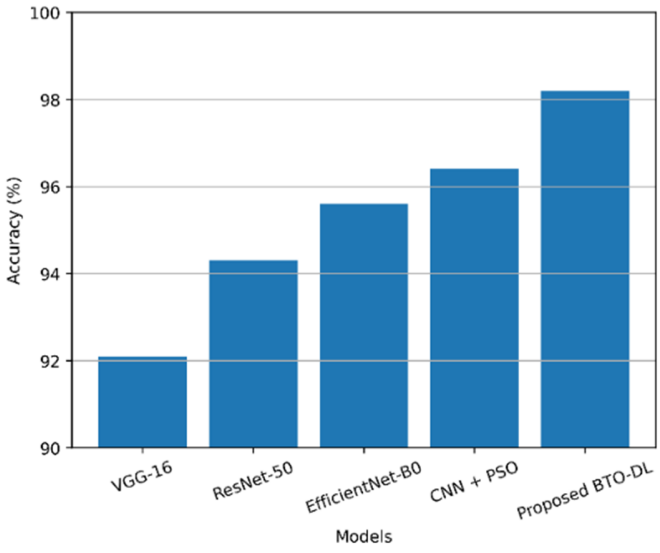

Fig. 1. Comparison of model accuracy on the Figshare Brain MRI dataset.

TABLE I. PERFORMANCE COMPARISON ON FIGSHARE BRAIN MRI DATASET

Model	Accuracy (%)	Precision (%)	Recall (%)	F1-score (%)
VGG-16	92.1	91.4	90.8	91.1
ResNet-50	94.3	93.9	93.1	93.5
EfficientNet-B0	95.6	95.1	94.7	94.9
CNN + PSO	96.4	96.1	95.8	95.9
Proposed BTO-DL	98.2	97.9	97.6	97.7

TABLE II. BINARY CLASSIFICATION RESULTS ON KAGGLE MRI DATASET

Model	Accuracy (%)	F1-score (%)	AUC
AlexNet	93.4	92.8	0.956
DenseNet-121	95.9	95.4	0.973
CNN + GA	96.7	96.2	0.981
Proposed BTO-DL	98.8	98.3	0.994

TABLE III. CLASS-WISE PERFORMANCE ON FIGSHARE BRAIN DATASET

Tumor type	Precision (%)	Recall (%)	F1-score (%)
Glioma	97.5	97.2	97.3
Meningioma	98.4	98.1	98.2
Pituitary	99.1	98.9	99.0
Normal	97.9	97.6	97.7

For fair comparison, all baseline models (VGG-16, ResNet-50, EfficientNet-B0, CNN+PSO, and CNN+GA) were trained and evaluated under identical experimental settings. Each model used the same patient-independent 70%/15%/15% train/validation/test split, identical preprocessing (z-score normalization and Gaussian smoothing), and a fixed training duration of 50 epochs. Hyperparameters of baseline CNN models were tuned using standard grid search, whereas PSO and GA variants optimized only network hyperparameters. The proposed BTO-DL framework jointly optimized CNN hyperparameters (learning rate, kernel size, number of filters, and dropout ratio) and deep feature importance weights. Performance metrics, including accuracy, precision, recall, F1-score, Receiver Operating Characteristic–Area Under the Curve (ROC–AUC), and Dice coefficient, were computed on the same held-out test sets.

An ablation study was conducted to evaluate the contribution of each component of the proposed framework, and the results are shown in Table IV. In addition, Table V shows that the proposed BTO-DL framework achieved the highest Dice coefficient of 0.91. Representative visualization examples are provided in Figure 2.

TABLE IV. ABLATION ANALYSIS

Configuration	Accuracy (%)
CNN only	94.8
CNN + feature weighting	96.1
CNN + BTO (hyperparameters only)	97.3
CNN + BTO (full model)	98.2

TABLE V. DICE COEFFICIENT COMPARISON ON BRATS DATASET

Model	Dice coefficient
U-Net	0.84
Attention U-Net	0.87
ResNet-based CNN	0.88
CNN + PSO	0.89
CNN + GA	0.90
Proposed BTO-DL	0.91

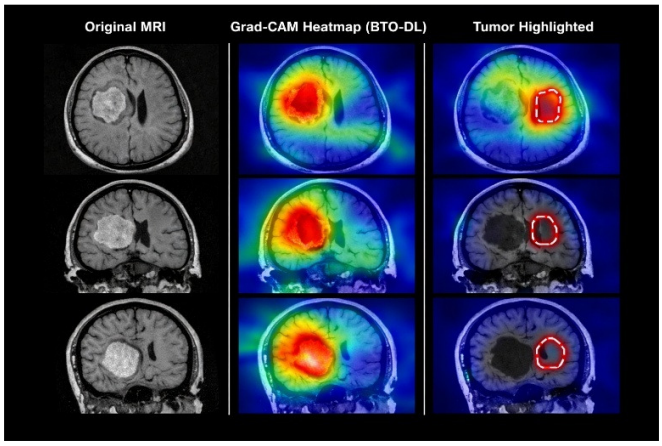

Fig. 2. Grad-CAM visualization results for representative MRI samples.

1) Computational Efficiency and Statistical Significance

The average time per MRI slice was 18.6 ms, comparable to conventional CNN-based models and significantly faster than deeper architectures such as ResNet-50 (≈24.3 ms per slice). The computational complexity of the proposed framework is $O(N \times I \times F)$, where N denotes the BTO population size, I is the number of iterations, and F represents the CNN forward-backward cost. Although metaheuristic optimization introduces additional overhead, this is limited to the training phase. Finally, a statistical significance test was performed to assess the reliability of the observed improvements in performance. The results indicate that the enhancements of the proposed BTO-DL framework over baseline models are significant ($p < 0.01$).

2) Comparison with Previously Published Methods

Table VI presents a comparative analysis of the proposed BTO-DL framework with previously published methods on the Figshare and Kaggle datasets.

TABLE VI. COMPARISON WITH PREVIOUSLY PUBLISHED WORKS ON FIGSHARE BRAIN AND KAGGLE DATASETS

Method	Dataset	Accuracy (%)
Transfer CNN [8]	Figshare	92–95
EfficientNet [8]	Figshare	95–96
Proposed BTO-DL	Figshare	98.2
AlexNet–GRU [10]	Kaggle	93–95
DenseNet [11]	Kaggle	95–97
Proposed BTO-DL	Kaggle	98.8

IV. CONCLUSION

This work introduces a unified optimization framework that simultaneously tunes Convolutional Neural Network (CNN) hyperparameters and deep feature importance using Bluefin Trevally Optimization (BTO). Unlike prior metaheuristic-assisted approaches that optimize only architectural parameters, the proposed framework jointly enhances feature representation and classification performance, resulting in improved Dice coefficient, Receiver Operating Characteristic–Area Under the Curve (ROC–AUC), and convergence robustness.

The framework uses BTO's adaptive exploration and exploitation strategies to address the limitations of manually tuned deep learning models, improving convergence stability and generalization capability. The BTO-based Deep Learning (BTO-DL) framework demonstrated accurate tumor classification and localization, achieving a classification accuracy of over 98%, ROC–AUC values close to 0.99, and a Dice coefficient of 0.91 on the BraTS dataset. Future work will focus on incorporating attention-driven explainability modules and extending the framework to 3D volumetric Magnetic Resonance Imaging (MRI) analysis to further improve clinical transparency and diagnostic reliability.

REFERENCES

[1] A. K. Budati and R. B. Katta, "An automated brain tumor detection and classification from MRI images using machine learning techniques with IoT," *Environment, Development and Sustainability*, vol. 24, no. 9, pp. 10570–10584, Sept. 2022, https://doi.org/10.1007/s10668-021-01861-8.

[2] M. Rasool, A. Noorwali, H. Ghandorh, N. A. Ismail, and W. M. S. Yafooz, "Brain Tumor Classification using Deep Learning: A State-of-the-Art Review," *Engineering, Technology & Applied Science Research*, vol. 14, no. 5, pp. 16586–16594, Oct. 2024, https://doi.org/10.48084/etasr.8298.

[3] A. Martín-Pérez *et al.*, "Hyperparameter Optimization for Brain Tumor Classification with Hyperspectral Images," in *2022 25th Euromicro Conference on Digital System Design*, Maspalomas, Spain, 2022, pp. 835–842, https://doi.org/10.1109/DSD57027.2022.00117.

[4] Y. A. Kadhim, M. S. Guzel, and A. Mishra, "A Novel Hybrid Machine Learning-Based System Using Deep Learning Techniques and Meta-Heuristic Algorithms for Various Medical Datatypes Classification," *Diagnostics*, vol. 14, no. 14, July 2024, Art. no. 1469, https://doi.org/10.3390/diagnostics14141469.

[5] M. M. Ahmed *et al.*, "Brain tumor detection and classification in MRI using hybrid ViT and GRU model with explainable AI in Southern Bangladesh," *Scientific Reports*, vol. 14, no. 1, Oct. 2024, Art. no. 22797, https://doi.org/10.1038/s41598-024-71893-3.

[6] R. Disci, F. Gurcan, and A. Soylu, "Advanced Brain Tumor Classification in MR Images Using Transfer Learning and Pre-Trained Deep CNN Models," *Cancers*, vol. 17, no. 1, Jan. 2025, Art. no. 121, https://doi.org/10.3390/cancers17010121.

[7] R. B. Vure and L. K. Pappala, "Enhanced brain tumor classification framework using deep learning," *Scientific Reports*, vol. 15, no. 1, Oct. 2025, Art. no. 35814, https://doi.org/10.1038/s41598-025-19882-y.

[8] C. Sankari, V. Jamuna, and A. R. Kavitha, "Hierarchical multi-scale vision transformer model for accurate detection and classification of brain tumors in MRI-based medical imaging," *Scientific Reports*, vol. 15, no. 1, Oct. 2025, Art. no. 38275, https://doi.org/10.1038/s41598-025-23100-0.

[9] Y. Wong, E. L. M. Su, C. F. Yeong, W. Holderbaum, and C. Yang, "Brain tumor classification using MRI images and deep learning techniques," *PLOS ONE*, vol. 20, no. 5, May 2025, Art. no. e0322624, https://doi.org/10.1371/journal.pone.0322624.

[10] A. Priya and V. Vasudevan, "Brain tumor classification and detection via hybrid alexnet-gru based on deep learning," *Biomedical Signal Processing and Control*, vol. 89, Mar. 2024, Art. no. 105716, https://doi.org/10.1016/j.bspc.2023.105716.

[11] R. Khan *et al.*, "High-precision brain tumor classification from MRI images using an advanced hybrid deep learning method with minimal radiation exposure," *Journal of Radiation Research and Applied Sciences*, vol. 18, no. 4, Dec. 2025, Art. no. 101858, https://doi.org/10.1016/j.jrras.2025.101858.

[12] P. Zhang, Z. Wei, C. Che, and B. Jin, "DeepMGT-DTI: Transformer network incorporating multilayer graph information for Drug–Target interaction prediction," *Computers in Biology and Medicine*, vol. 142, Mar. 2022, Art. no. 105214, https://doi.org/10.1016/j.compbiomed.2022.105214.

[13] P. Afshar, A. Mohammadi, and K. N. Plataniotis, "Brain Tumor Type Classification via Capsule Networks," in *2018 25th IEEE International Conference on Image Processing*, Athens, Greece, 2018, pp. 3129–3133, https://doi.org/10.1109/ICIP.2018.8451379.

[14] M. Toğaçar, B. Ergen, and Z. Cömert, "Tumor type detection in brain MR images of the deep model developed using hypercolumn technique, attention modules, and residual blocks," *Medical & Biological Engineering & Computing*, vol. 59, no. 1, pp. 57–70, Jan. 2021, https://doi.org/10.1007/s11517-020-02290-x.

[15] P. K. Ramtekkar, A. Pandey, and M. K. Pawar, "Accurate detection of brain tumor using optimized feature selection based on deep learning techniques," *Multimedia Tools and Applications*, vol. 82, no. 29, pp. 44623–44653, Dec. 2023, https://doi.org/10.1007/s11042-023-15239-7.

[16] T. M. Hasan and J. Alneamy, "Medical Images Classification Using Hybrid Deep Learning CNN-PSO-GA," in *2022 8th International Conference on Contemporary Information Technology and Mathematics*, Mosul, Iraq, 2022, pp. 90–95, https://doi.org/10.1109/ICCITM56309.2022.10031978.

[17] S. Mirjalili, S. Saremi, S. M. Mirjalili, and L. dos S. Coelho, "Multi-objective grey wolf optimizer: A novel algorithm for multi-criterion optimization," *Expert Systems with Applications*, vol. 47, pp. 106–119, Apr. 2016, https://doi.org/10.1016/j.eswa.2015.10.039.

[18] X. Liu, L. Song, S. Liu, and Y. Zhang, "A Review of Deep-Learning-Based Medical Image Segmentation Methods," *Sustainability*, vol. 13, no. 3, Jan. 2021, Art. no. 1224, https://doi.org/10.3390/su13031224.

[19] B. H. Menze *et al.*, "The Multimodal Brain Tumor Image Segmentation Benchmark (BRATS)," *IEEE Transactions on Medical Imaging*, vol. 34, no. 10, pp. 1993–2024, Oct. 2015, https://doi.org/10.1109/TMI.2014.2377694.

[20] "brain tumor dataset." figshare, Apr. 02, 2017, https://doi.org/10.6084/m9.figshare.1512427.v8.

[21] "Brain MRI Images for Brain Tumor Detection." Kaggle. [Online]. Available: https://www.kaggle.com/datasets/navoneel/brain-mri-images-for-brain-tumor-detection.